Localization of Nuclear Subunits of Cyclic AMP-dependent Protein Kinase by the Immunocolloidal Gold Method

MICHAEL R. KUETTEL,* STEPHEN P. SQUINTO,* JOANNA KWAST-WELFELD,* GERHILD SCHWOCH,‡ JOHN S. SCHWEPPE,* and RICHARD A. JUNGMANN*

*Department of Molecular Biology, Northwestern University Medical School, Chicago, Illinois 60611, and ‡Abteilung für Klinische Biochemie, Universität Göttingen, Göttingen, Federal Republic of Germany

ABSTRACT An immunocolloidal gold electron microscopy method is described allowing the ultrastructural localization and quantitation of the regulatory subunits RI and RII and the catalytic subunit C of cAMP-dependent protein kinase. Using a postembedding indirect immunogold labeling procedure that employs specific antisera, the catalytic and regulatory subunits were localized in electron-dense regions of the nucleus and in cytoplasmic areas with a minimum of nonspecific staining. Antigenic domains were localized in regions of the heterochromatin, nucleolus, interchromatin granules, and in the endoplasmic reticulum of different cell types, such as rat hepatocytes, ovarian granulosa cells, and spermatogonia, as well as cultured H4IIE hepatoma cells.

Morphometric quantitation of the relative staining density of nuclear antigens indicated a marked modulation of the number of subunits per unit area under various physiologic conditions. For instance, following partial hepatectomy in rats, the staining density of the nuclear RI and C subunits was markedly increased 16 h after surgery. Glucagon treatment of rats increased the staining density of only the nuclear catalytic subunit. Dibutyryl cAMP treatment of H4IIE hepatoma cells led to a marked increase in the nuclear staining density of all three subunits of cAMP-dependent protein kinase. These studies demonstrate that specific antisera against cAMP-dependent protein kinase subunits may be used in combination with immunogold electron microscopy to identify the ultrastructural location of the subunits and to provide a semi-quantitative estimate of their relative cellular density.

Cyclic AMP (cAMP) is the intracellular mediator of the regulatory signal of several polypeptide hormones and catecholamines. It plays a key role in the modulation of nuclear events such as the specific regulation of transcription of a number of cAMP-induced enzymes and proteins (1–4), phosphorylation/dephosphorylation of histones and nonhistone chromosomal proteins (5, 6), and nuclear mechanisms that may be involved in cAMP-regulated control of cellular proliferation (7). However, the precise sequence of molecular steps initiated by cAMP in these nuclear events remains to be elucidated. From our present knowledge of cAMP action it appears that cAMP-dependent protein kinase, the only identified mediator of cAMP action in eukaryotic cells, forms an important link in these nuclear events. Two isoenzyme forms of cAMP-dependent protein kinase (type I and type II) are found in mammalian tissues in various ratios depending on the cell type (8). These tetrameric holoenzymes contain a regulatory subunit dimer (R_2) and two catalytic subunits (C) (9, 10). The type I and type II isoenzymes differ only in their regulatory subunits (RI and RII) which both are the major cAMP-binding proteins in eukaryotic cells identified so far. The potential relevance of the cAMP-dependent protein kinases to the understanding of differentiation and cellular growth is suggested by findings that the relative amounts of type I and type II isoenzymes change at times of physiological transitions (11–16) implying selective regulatory roles for the RI and RII subunits.

Although the cAMP-mediated nuclear events imply a functional association of protein kinase subunits with nuclear components, it is difficult to unambiguously identify a nuclear location of cAMP-dependent protein kinase subunits by clas-

[1] Abbreviations used in this paper: PEG-GMA, polyethylene glycol-glycol methacrylate mix; TBS, 3% bovine serum albumin in 0.05 M Tris, pH 7.5, 0.2 M NaCl.

sical biochemical techniques involving cell homogenization and differential centrifugation. Possible perturbation of cellular structure during homogenization, the common use of nonphysiological homogenization media, and the susceptibility of the cytosol to protein kinase subunit redistribution during subcellular fractionation make an unequivocal demonstration of the presence or interaction of protein kinase subunits with the nucleus technically difficult. A valuable complementary approach to the problem of interaction and localization of protein kinase subunits within the cell is the application of histochemical or immunocytochemical techniques. With the introduction of immunoglobulin-linked colloidal gold solutions (17) the localization and quantitation of antigen–antibody complexes has been greatly facilitated (18–22). Sufficiently electron-dense to be readily visible in the nucleus (23–25), immunogold reagents may be used in nuclear antigen labeling studies. In this paper we report the nuclear localization of the catalytic and regulatory subunits of cAMP-dependent protein kinase and demonstrate the applicability of immunogold electron microscopy in the identification and localization of the subunits at discrete nuclear substructures and to provide a semi-quantitative estimate of their cellular density.

MATERIALS AND METHODS

Cell Culture: A cloned cell line (H4IIE) derived from Reuber H35 hepatoma was kindly provided by Dr. Daryl Granner (University of Iowa). The cells were grown as monolayer cultures in Swimm's 77 medium supplemented with 2.5% fetal calf serum, 2.5% newborn calf serum, 50 U/ml of penicillin, 50 μg/ml of streptomycin, 2.4 mM $CaCl_2$, 60 mM cystine, and 60 mM *N*-(2-hydroxy-1-1-bis[hydroxymethyl]ethyl) glycine. The cells were subcultured at confluency by trypsinization. Cells from a single 850-cm^2 roller bottle were scraped into 5 ml of serum-free Swimm's 77 and pelleted by centrifugation at 4°C. The serum-free medium was decanted and 5.0 ml of 2.5% glutaraldehyde in 0.1 M sodium phosphate, pH 7.4, was added to ~0.2 ml of cell pellet. The cells were resuspended by gentle agitation. After 1 h, cells were recovered by centrifugation. The glutaraldehyde solution was decanted and the cells were washed in 0.1 M sodium phosphate/7% sucrose for 10 min before repelleting. Cells were dehydrated with ethanol and embedded in a low viscosity resin according to the method of Spurr (26).

Preparation of Tissues: Liver, ovaries, and testes were taken from adult Sprague-Dawley rats (150–200 g) that had been killed by cervical dislocation. Small tissue sections (~1 mm^3) were fixed according to the protocols given in the text (see Tables I and II). After fixation, the tissue sections were dehydrated in ethanol, and embedded in a low viscosity resin (26). The embedding plastic had no effect on the distribution of immunogold staining using all three antisera (Tables I and II).

Preparation of Tissue Sections and Staining Protocol: Thin sections (70–80-nm thick) were cut on an ultramicrotome and mounted on 200-mesh nickel grids. To localize antigens, we processed mounted tissue sections by an indirect immunogold staining method similar to ones previously described (18, 27–29). All grids were floated with the tissue section face down on 50-μl drops at room temperature. Mounted tissue sections were first etched with 10% H_2O_2 for 10 min to enhance immunostaining (30–31). After a rinse in distilled water, nonspecific sites of protein absorption were blocked with a 1:100 dilution of normal goat serum in PBS for 5 min. After the blocking step, the grids were incubated for 60 min with the respective antiserum or preimmune serum diluted in PBS as indicated in the text. After a rinse in PBS, the grids were floated for 30 min on a 1:2 dilution of goat anti-rabbit immunoglobulin linked to 20-nm colloidal gold particles (Janssen Pharmaceuticals, Beerse, Belgium). After a rinse with phosphate-buffered saline (PBS), nuclear morphology was enhanced by staining with 3% aqueous uranyl acetate for 10 min followed by lead citrate for 5 min (32). The sections were examined using a JEOL JEM-100 CX electron microscope operated at 80 keV and photographed with Kodak 4489 EM film.

Quantitative Evaluation by Morphometric Analysis: Morphometric quantitation of immunogold staining was carried out in at least 10 different cells from each of three different immunogold preparations. Each micrograph was photographed at an initial magnification of 7,200 and analyzed at a final magnification of 72,000 by placing each micrograph negative in an optical enlarging bench equipped with a Numonics digitizer operated with a Hewlett-Packard 9820A computer programmed to record the number of gold particles per unit area. Immunogold labeling is expressed as the number of colloidal gold particles per cellular component unit area.

Purification of Antigen: The regulatory subunits RI and RII were prepared and purified from rat liver according to Dills et al. (33). Bovine catalytic subunit was purified as described previously (34).

Preparation and Characterization of Antisera: Preparation of the antiserum against bovine heart catalytic subunit in rabbits and its characterization and cross-reactivity with rat liver catalytic subunit have been described (34, 35). Antisera against rat liver regulatory subunits RI and RII were prepared in rabbits using highly purified RI and RII. Non-immune control

TABLE I. *Staining Intensity in Rat Hepatocytes Obtained for the Catalytic Subunit of cAMP-dependent Protein Kinase Using Different Fixation Conditions*

Fixation	Postfixation	Media	Intensity of labeling (gold particles/μm^2 ± SEM)		
			Nucleus	Cytoplasm	Sinusoid
2.5% Glutaraldehyde	1% OsO_4	Spurr	16.3 ± 1.4	15.9 ± 1.3	2.5 ± 0.2
2.5% Glutaraldehyde	—	Spurr	39.8 ± 1.2	23.0 ± 1.0	2.5 ± 0.2
2.5% Glutaraldehyde	1% OsO_4	PEG-GMA	ND		
1.0% Glutaraldehyde	—	Spurr	20.5 ± 2.2	15.4 ± 1.2	1.1 ± 0.2
1.0% Glutaraldehyde	—	PEG-GMA	ND		
4.0% Paraformaldehyde + 0.5% Glutaraldehyde	—	Spurr	9.1 ± 1.0	9.7 ± 1.1	1.3 ± 0.1
Dimethylsuberimidate (20 mg/ml)	1% OsO_4	Spurr	11.3 ± 0.8	12.5 ± 0.2	0.8 ± 0.1
Dimethylsuberimidate (20 mg/ml)	—	Spurr	9.0 ± 0.7	6.9 ± 1.3	1.1 ± 0.1
Embedding medium alone		Spurr	0.3 ± 0.1		

ND, not determined because of high nonspecific binding over resin.
Rat liver tissue sections were fixed as indicated and processed by staining with anti-C serum.

TABLE II. *Staining Intensity Obtained for the Regulatory Subunits RI and RII of cAMP-dependent Protein Kinase in Rat Hepatocytes*

Subunit	Fixation	Intensity of labeling (gold particles/μm^2 ± SEM)			Embedding medium
		Nucleus	Cytoplasm	Sinusoid	
RI	2.5% Glutaraldehyde	39.8 ± 1.4	49.1 ± 3.3	2.9 ± 0.2	
RII	2.5% Glutaraldehyde	27.2 ± 1.7	31.6 ± 1.7	2.4 ± 0.3	
RI					0.2 ± 0.1
RII					0.3 ± 0.1

immunoglobulins were prepared by the same method from sera of uninjected rabbits. Affinity purification of the antisera was carried out as described by Miles et al. (36). The specificity of the antisera was tested extensively by Ouchterlony double-diffusion analysis (37), double-antibody precipitation, indirect enzyme-linked immunosorbent assay (ELISA) (35), and immunoblot analysis (38).

Immunoblot Analysis: Purified antigens and either whole cell protein or nuclear protein extracts were subjected to electrophoresis on SDS 10% polyacrylamide gels (39). The proteins were transferred to nitrocellulose paper (38) using an Electroblot apparatus (E-C Apparatus Corp., St. Petersburg, FL). Experiments were carried out to determine the efficiency of protein transfer using [^{35}S]methionine-labeled H4IIE cytosol. After 3 h of electroblotting, we observed complete transfer of the soluble ^{35}S-labeled proteins from the gel to the nitrocellulose membrane (see Fig. 2). After electroblotting, the nitrocellulose membrane was stored overnight at 4°C in transfer buffer (0.025 M Tris, pH 8.3, 0.192 M glycine, and 20% methanol [vol/vol]). Remaining protein binding sites on the membrane were blocked with 3% bovine serum albumin in 0.05 M Tris, pH 7.5, and 0.2 M NaCl (TBS) for 1 h at room temperature using gentle agitation. After blocking, the membrane was placed into a primary antibody solution (anti-RI [1:100], anti-RII [1:100], or anti-C [1:250] in TBS) for 24 h at 4°C with gentle agitation. The membrane was then washed three times in TBS containing 0.1% Tween 20 (15 min/wash). Identification of antigen was carried out using the BRL Immunodetection Kit (Bethesda Research Laboratories Inc., Rockville, MD). Accordingly, secondary antibody (affinity-purified biotinylated goat anti-rabbit IgG) was diluted to 3 μg/ml in TBS. The membrane was incubated in secondary antibody solution for 1 h at room temperature using gentle agitation. After incubation, the membrane was washed three times in TBS and placed in a solution of streptavidin-HRP enzyme conjugate (diluted 1:500 in TBS) for 30 min at room temperature. The membrane was again washed three times in TBS and then immersed into substrate solution (0.5 mg/ml of 4-chloro-1-naphthol in TBS). The membrane was incubated in substrate solution without agitation at room temperature for 30 to 60 min or until a blue-purple color was observed indicating antibody-antigen conjugation.

RESULTS

Analysis of Antisera

The preparation and characterization of antiserum against bovine heart catalytic subunit and its cross-reactivity with rat liver catalytic subunit have been described in detail (34, 35) Antisera against rat liver regulatory subunits RI and RII were raised in rabbits by injecting them with purified antigen using an identical procedure. The specificities of the antisera were determined in several ways. Double immunodiffusion Ouchterlony analysis of the antisera and purified rat liver RI, RII, or C and crude rat liver 105,000 *g* supernatant fraction showed in each case a single continuous immunoprecipitation band (results not shown). This suggested the presence of a single antibody-antigen system. For the competitive ELISA, the RI and RII antisera were preincubated with either RI or RII and then added to the antigen-coated microtiter wells. As shown in Fig. 1, only the complementary antigen eliminated the reactivity of the respective antiserum toward RI or RII. The noncomplementary antigen did not compete even at 100-fold the concentration of complementary antigen with which competition was first detected. Western blot analysis of the affinity-purified RI, RII, and C antisera showed that all three specifically reacted with their complementary antigen in a whole cell protein extract from rat liver, ovary, or H4IIE cells (Fig. 2, *lower panels, A–C*). Preimmune serum showed no reactivity (Fig. 2, *lower panels, D*). Similarly, all three antisera reacted with their complementary antigen in a rat liver nuclear protein extract (Fig. 3) and only minor apparent nonspecific bands are detected (the peak with the shoulder in scan *E* represents the phospho- and dephosphoforms of RII). It is important to note that Western blot analysis was done using either a 1:100 dilution (anti-RI or anti-RII) or a 1:250 dilution (anti-C) of antiserum, whereas immunogold antigen detection

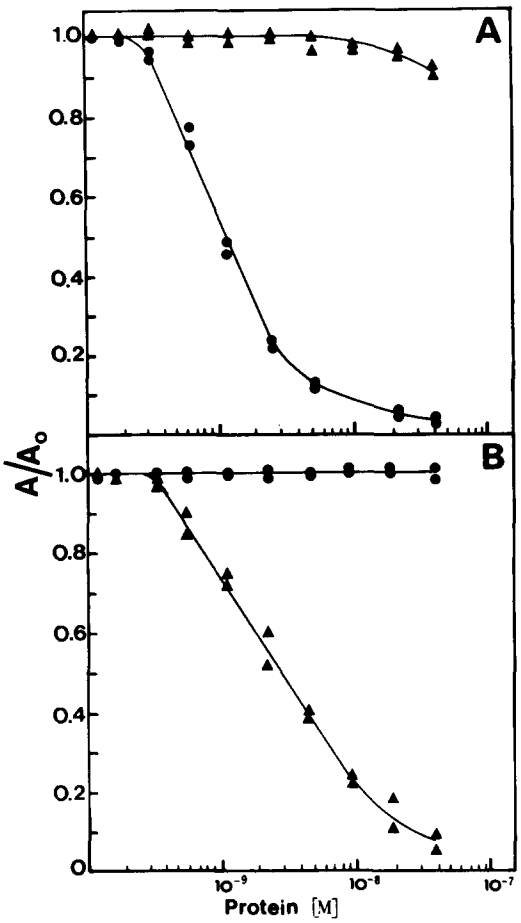

FIGURE 1 Competitive ELISA of RI and RII antibodies. Detection of antibody activity against rat liver regulatory subunits RI and RII was with an alkaline phosphatase goat anti-rabbit IgG conjugate and *p*-nitrophenyl phosphate substrate as described in detail previously (34). Microtiter wells were coated with 5 ng/well of purified rat liver RI (*A*) or rat liver RII (*B*). The wells were then incubated with RI and RII antisera that had been preincubated with the indicated concentrations of either RI or RII. Anti-RI and anti-RII sera were used at a dilution of 1:16,000. All points are means of duplicate determinations. (*A*) Anti-RI preincubated with RI (●) or RII (▲). (*B*) Anti-RII preincubated with RI (●) or RII (▲).

was done with a substantially greater dilution of antiserum, further diluting out any potential cross-reacting contaminating antibodies.

Effect of Tissue Fixation

The labeling intensity on thin sections fixed under various conditions is presented in Tables I and II. Best results were obtained with a fixation protocol including 2.5% glutaraldehyde and elimination of osmium tetroxide. Intense, specific staining was obtained with 2.5% glutaraldehyde as fixative in nuclear and cytoplasmic areas, whereas only negligible labeling was found in sinusoidal areas or the embedding medium alone. The optimal dilutions of the antisera and corresponding preimmune sera for a 60-min incubation time with the tissue sections were 1:500 for the catalytic subunit antiserum and 1:2,000 for the RI and RII regulatory subunit antisera. Higher concentrations usually led to an increase of nonspecific background labeling. Counterstaining of thin sections with uranyl acetate and lead citrate did not affect the staining intensity (data not shown). For polyethylene glycol-glycol methylacry-

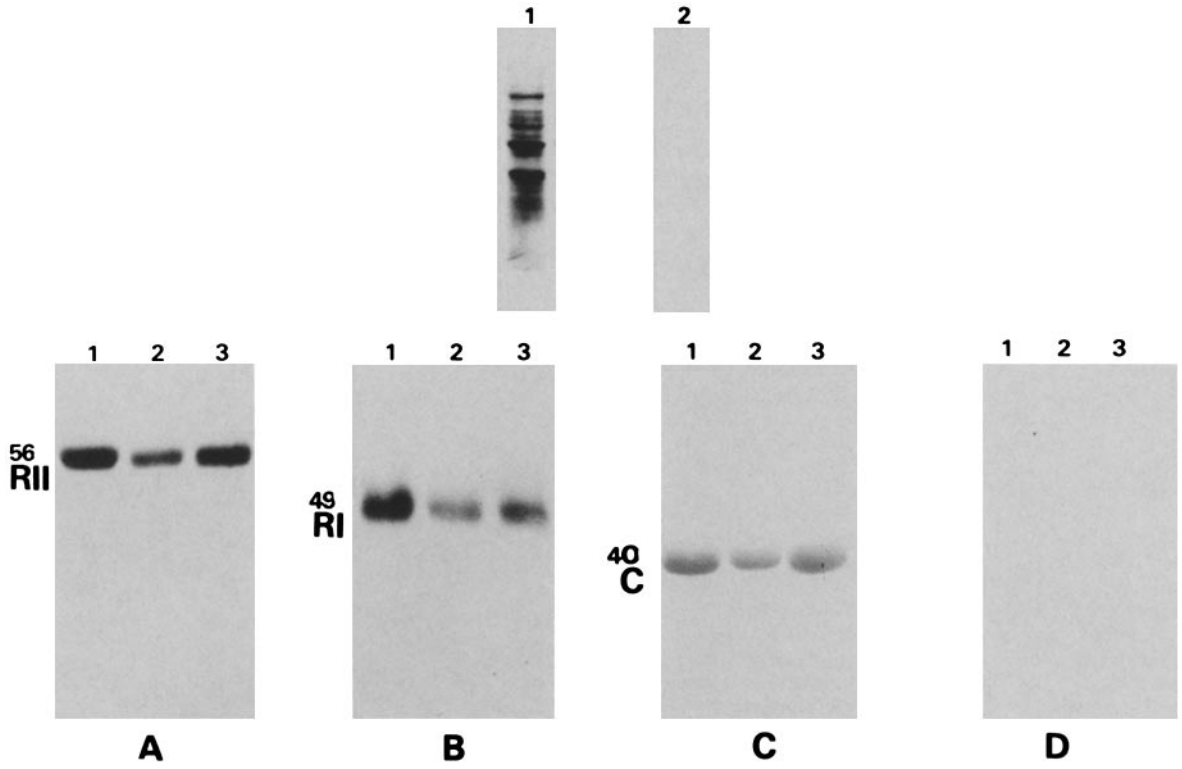

FIGURE 2 Analysis of antibody specificity by immunoblotting. (*Upper panels*) Protein transfer to nitrocellulose. H4IIE cells were incubated with 50 μCi of [^{35}S]methionine for 24 h. Cytosol protein was prepared, resolved on SDS 10% polyacylamide gels, and transferred to nitrocellulose by electroblotting. The blotted gel and nitrocellulose membrane were dried and placed on a Kodak X-omat XRP-5 film for 3 d to obtain autoradiographs. The transferred ^{35}S-labeled proteins are shown in lane *1*. Labeled proteins remaining in the gel after blotting are shown in lane *2*. (*Lower panels*) Immunodetection of protein kinase subunits. Whole cell extracts from rat liver, rat ovary, or cultured H4IIE cells were separated by electrophoresis on SDS 10% polyacrylamide gels and transferred to nitrocellulose by electroblotting. Soluble proteins resolved by electrophoresis from rat liver (lane *1*), H4IIE cells (lane *2*), and rat ovary (lane *3*) were incubated with a 1:100 dilution of either anti-RII (*A*), anti R-I (*B*), a 1:250 dilution of anti C (*C*), or preimmune serum (*D*). Immunocomplexes were visualized with the BRL immunodetection kit as described in Materials and Methods. The molecular weights (× 10^3) of RI, RII, and C are indicated and were determined using standard protein markers.

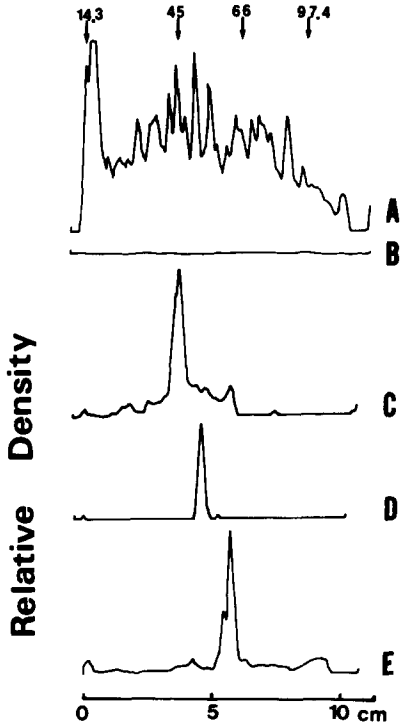

FIGURE 3 Laser beam densitometric scans of nuclear protein immunoblot autoradiograms. Rat liver nuclear 0.35 M NaCl extracts, prepared as described previously (*7*), were separated by electrophoresis on 10% polyacrylamide gels and transferred to nitrocellulose by electroblotting. Scan *A* was stained for protein with Amido black. The additional scans were incubated with a 1:100 dilution of either preimmune serum (*B*), anti-C (*C*), anti-RI (*D*), or anti-RII (*E*). Immunocomplexes were visualized with the BRL immunodetection kit as described in Materials and Methods. The molecular weights (× 10^3) of standard protein markers are indicated at the top of the figure.

late (PEG-GMA)–embedded thin sections, staining of all cellular structures was always accompanied with high background staining over the resin which was not the case when Spurr's embedding medium was used (Table I).

Controls for Specificity of Immunogold Staining

Three different types of controls were performed to test for the specificity of immunogold labeling. (*a*) After preincubation of thin sections with IgG from the respective preimmune sera followed by colloidal gold–linked goat anti-rabbit immunoglobulin only minimal immunogold staining was observed (Fig. 4*c*). (*b*) Almost complete abolition of staining was observed after preincubation of thin sections with the respective antigen or direct application of the colloidal gold–linked goat anti-rabbit immunoglobulin (micrographs not shown). (*c*) Finally, preabsorption of antiserum with excess

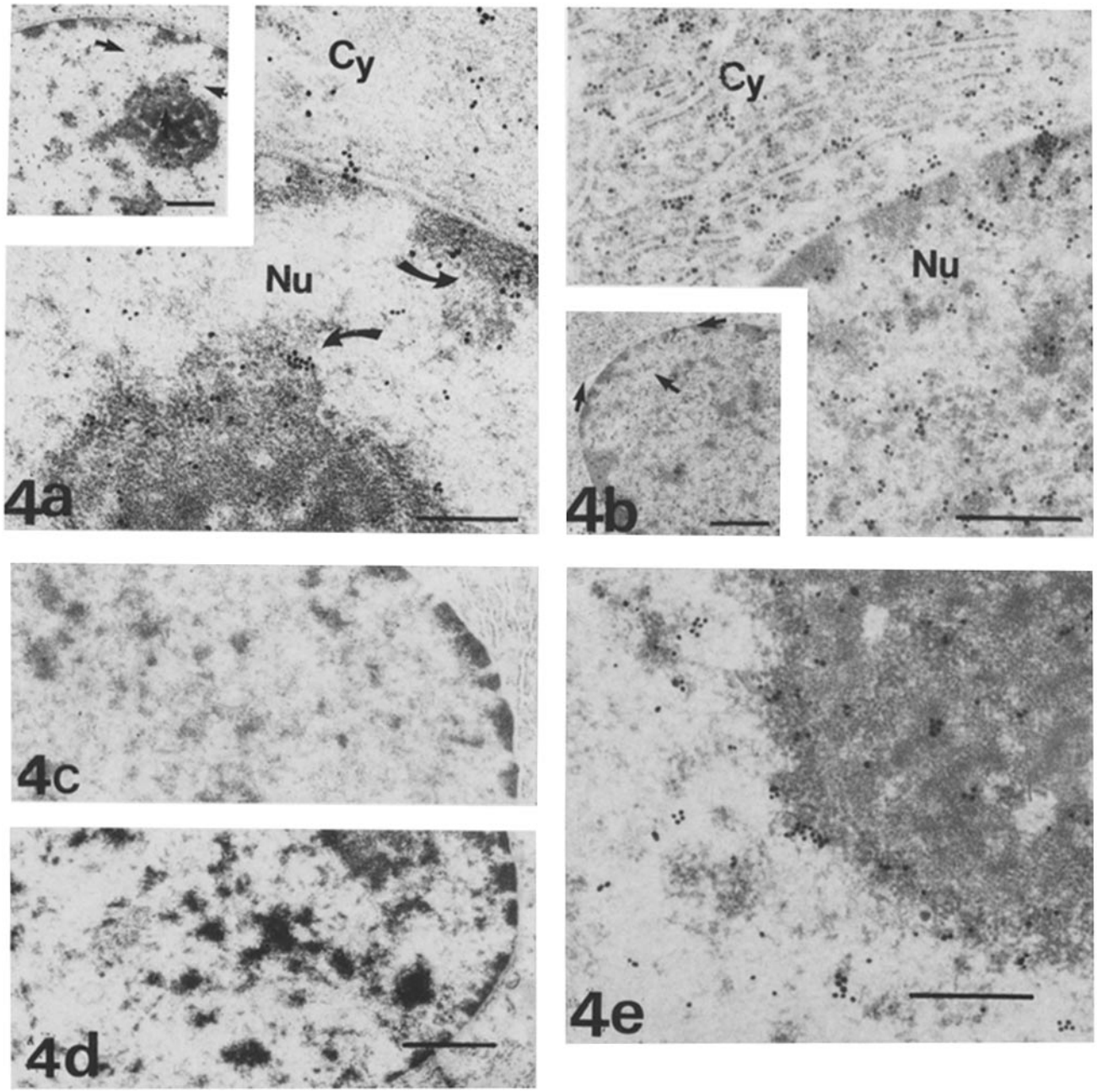

FIGURE 4 Immunogold electron micrographs of hepatocytes stained for the catalytic subunit of cAMP-dependent protein kinase. Liver tissue thin sections were prepared from male Sprague-Dawley rats (150–200 g) that had received an intraperitoneal injection of either 0.1 ml of saline or 0.4 mg of glucagon (Eli Lilly & Co., Indianapolis, IN) for 2 h or had been partially hepatectomized for 16 h as described (7). Fixation of tissue was carried out with 2.5% glutaraldehyde and embedding was in low-viscosity resin according to the method of Spurr (26). (*a*) Micrograph of a hepatocyte from a saline-injected rat stained with anti-C serum. *Nu*, nuclear area; *Cy*, cytoplasmic area. (*Inset*) Low magnification showing preferential localization of the catalytic subunit over the peripheral area of the nucleolus. Arrows in the inset denote the region of higher magnification. Bar, 0.5 μm; × 43,000; (*inset*) bar, 1.0 μm; × 10,750. (*b*) Micrograph of a hepatocyte from a glucagon-treated rat. (*Inset*) Low magnification showing relatively dense catalytic subunit staining. Arrows in inset denote the region of higher magnification. Bar, 0.5 μm; × 51,600; (*inset*) bar, 1.0 μm; × 12,000. (*c*) Micrograph of a hepatocyte from a saline-injected rat. The tissue section was treated with pre-immune serum diluted 1:500. Note absence of immunostaining. × 41,000. (*d*) Micrograph of a hepatocyte from a saline-injected rat. The tissue section was stained with anti-C serum that had been incubated with excess purified catalytic subunit. Note absence of immunostaining. Bar, 1.0 μm. × 41,000. (*e*) Micrograph of nuclear area in a hepatocyte from a partially hepatectomized rat showing staining over nucleolus and in peripheral areas of the nucleolus. Bar, 0.5 μm; × 50,000.

complementary antigen and subsequent preincubation of thin sections efficiently blocked immunogold staining (see a representative example in Fig. 4*d*). In addition, binding of colloidal gold complexes to the embedding resin was evaluated over the sinusoidal lumen within liver tissue or over regions free of tissue and was found to be insignificant (see Tables I and II).

Subunit Staining and Distribution

The results of labeling thin sections derived from a variety

of rat tissues with gold are shown in Figs. 4–7. The well-described biochemical characteristics of the cAMP-dependent protein kinase in the tissues studied (7, 12, 16) made them an ideal choice for the immunogold labeling studies. The ultrastructural localization of the subunits was accomplished through the use of the specific antisera in combination with a 20-nm colloidal gold–linked goat anti-rabbit antibody. In Fig. 4 cytoplasmic and nuclear areas of a hepatocyte from either saline-treated (Fig. 4*a*) or glucagon-treated (Fig. 4*b*) rats are shown stained with anti-C. Immunogold staining was associated with the endoplasmic reticulum (see especially Fig. 4*b*), with heterochromatin and with nucleolar regions (see arrows in Fig. 4*a*). After glucagon treatment, a higher labeling density of catalytic subunit was observed within the nucleus (compare inset of Fig. 4*a* with inset of Fig. 4*b*), and to a lesser extent also in cytoplasmic regions. Association of catalytic subunit with the nucleolus and heterochromatin areas in hepatic nuclei from partially hepatectomized rats is shown in Fig. 4*e*. Immunostaining of catalytic subunit in euchromatin appeared at low levels in all hepatocyte nuclei examined.

The staining and distribution of the regulatory subunits RI and RII in hepatocytes from regenerating rat liver are shown in Fig. 5. Both regulatory subunits are located over the endoplasmic reticulum (Figs. 5, *a–c*) and over nuclear areas particularly in heterochromatin and nucleolar areas (Figs. 5, *a* and *b*) and perichromatin regions (Fig. 5*c*, arrows and higher magnification of this region shown in Fig. 5*d*).

Fig. 6 shows the localization of the catalytic and RII sub-

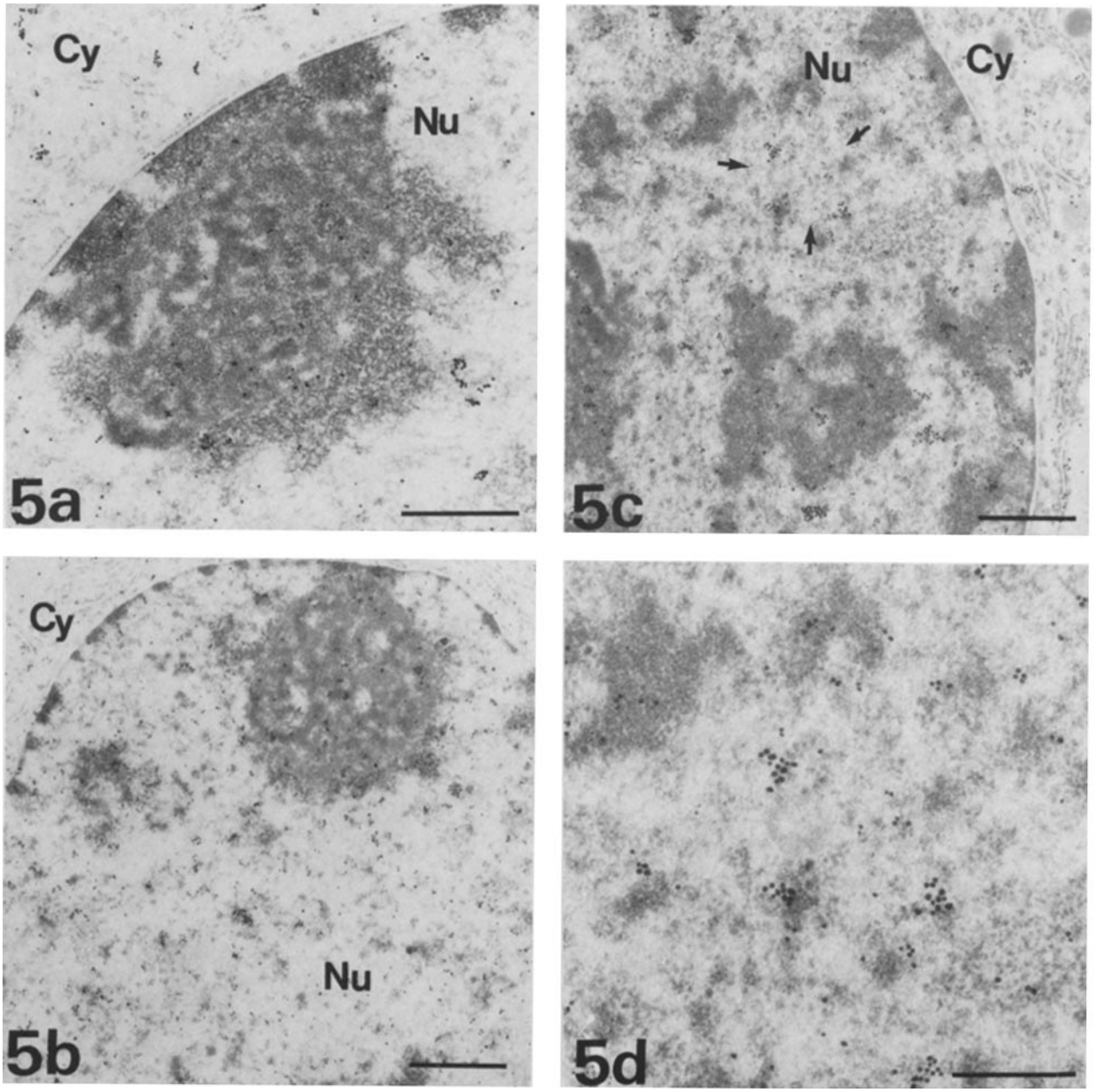

FIGURE 5 Immunogold electron micrographs of hepatocytes from regenerating liver stained for the regulatory subunits of RI and RII of cAMP-dependent protein kinase. (*a* and *b*) Micrographs of cytoplasmic (*Cy*) and nuclear (*Nu*) areas of hepatocytes stained with anti-RI serum from sham-operated (*a*) and partially hepatectomized (*b*) rats. (*c*) Hepatocyte stained with anti-RII serum from a partially hepatectomized rat. Arrows denote the region of higher magnification shown in *d*. Bars, (*a–c*) 1 μm; (*d*) 0.5 μm. (*a*) × 24,000; (*b*) × 21,000; (*c*) × 28,000; (*d*) 51,500.

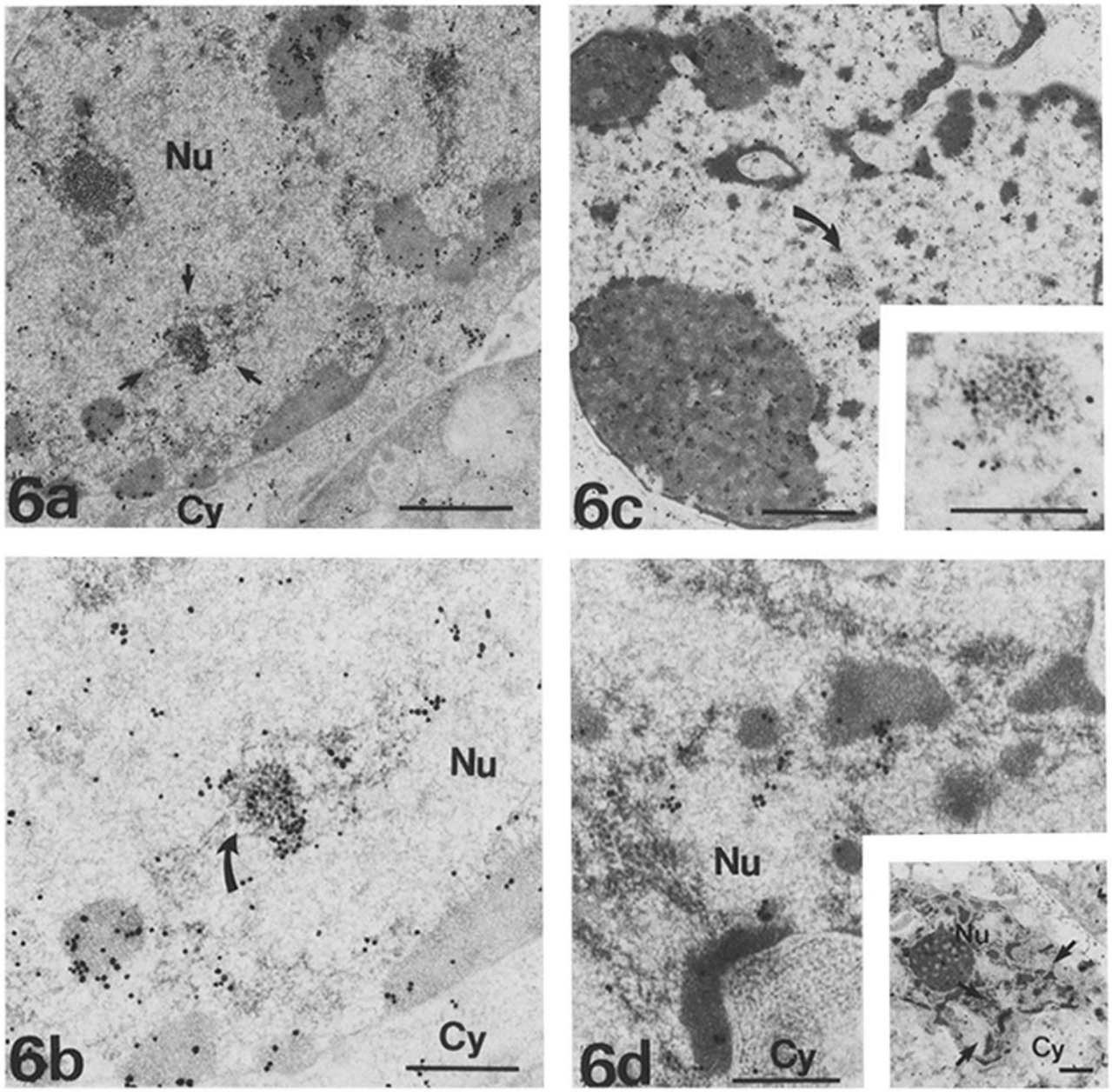

FIGURE 6 Immunogold electron micrographs of cultured H4IIE heptoma cells stained for the catalytic and RII subunits. (*a* and *b*) Untreated hepatoma cell stained with anti-C serum. Arrows denote region of higher magnification shown in b; arrow in *b* indicates relatively dense C subunit localization over area of interchromatin granules. (*a*) Bar, 1.0 μm; × 24,000; (*b*) bar, 0.5 μm; × 47,500. (*c*) Micrograph of nuclear area of hepatoma cell that had been treated with 0.5 mM dibutyryl cAMP for 10 min and stained with anti-C serum; arrow denotes area of higher magnification shown in inset showing catalytic subunit association with interchromatin granules. Bar, 1.0 μm; × 24,000; (*inset*) bar, 0.5 μm; × 56,100. (*d*) Higher magnification of untreated hepatoma cell stained with anti-RII serum. (*Inset*) Low magnification showing nuclear and cytoplasmic areas of hepatoma cell. Arrows in the inset mark the region of higher magnification. Bar, 0.5 μm; × 44,000; (*inset*) bar, 1 μm; × 7,200.

units in H4IIE hepatoma cells. These cells contain relatively low levels of type I cAMP-dependent protein kinase (Squinto, S. P., and Jungmann, R. A., unpublished observation) and RI staining in the nucleus was generally much lower than RII and C staining (see also Table IV). Regulatory subunit RII was distributed over cytoplasmic and nuclear areas (Fig. 6*d*, inset and higher magnification). The catalytic subunit showed a preferential association with nuclear areas, particularly with heterochromatin (Fig. 6*a*, top of micrograph) and with interchromatin granules (Fig. 6*a*, arrows, and higher magnification of that area shown in Fig. 6*b*). After dibutyryl cAMP treatment of H4IIE hepatoma cells, the catalytic subunit was distributed rather densely over heterochromatin (lower left corner of Fig. 6*c*) and over interchromatin granules (Fig. 6*c*, arrow and inset).

The subunit distribution was also examined in rat ovarian granulosa cells and rat spermatogonia. Fig. 7*c* shows a rather dense distribution of catalytic subunit in the heterochromatin and perichromatin region of the nucleus of a spermatogonium. The staining density in the cytoplasm, in contrast to nuclear areas, is considerably less. Rat granulosa cells show staining for the catalytic subunit (Fig. 7*a*), the regulatory

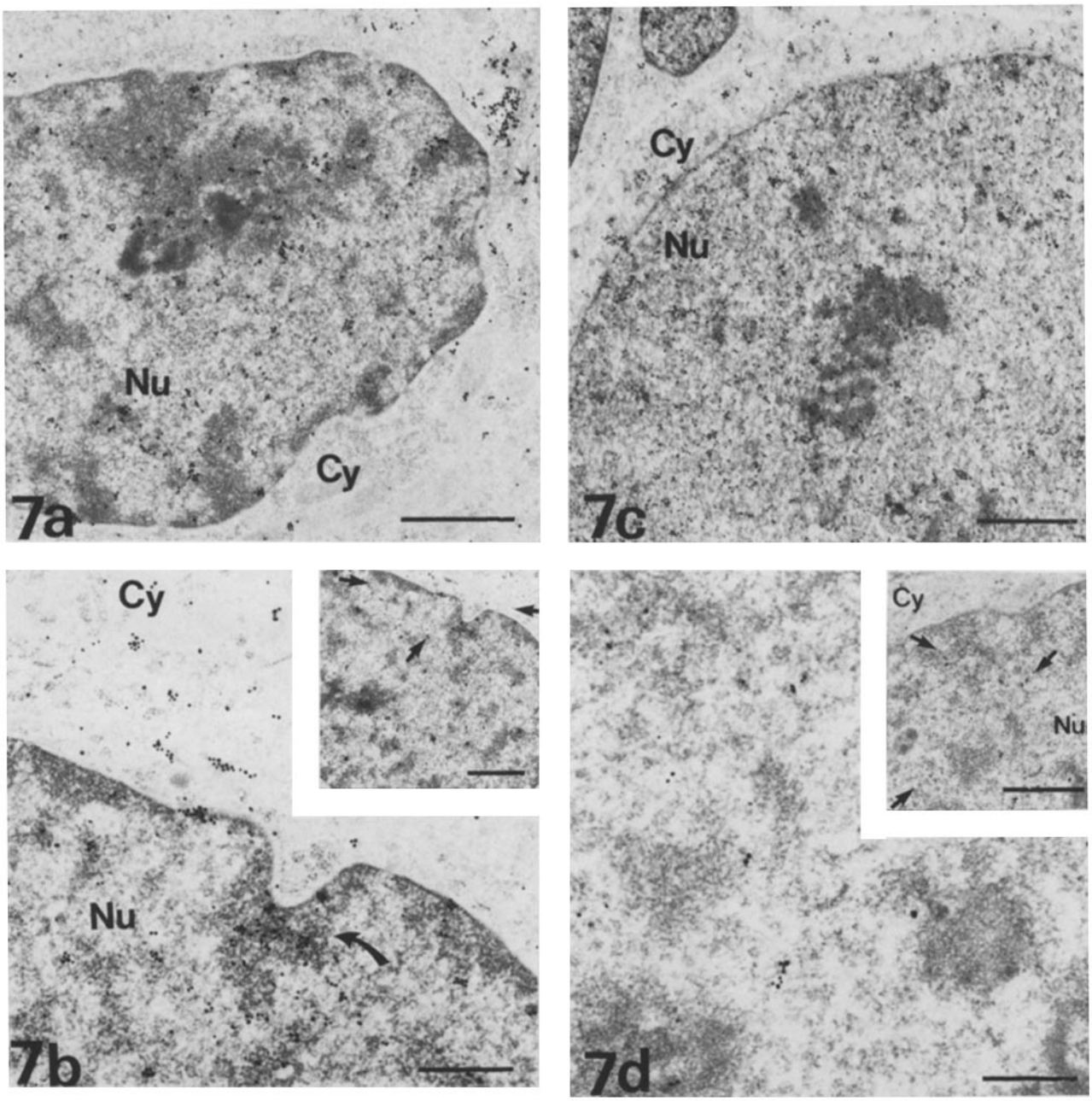

FIGURE 7 Immunogold electron micrographs of rat granulosa cells and spermatogonium. (*a*, *b*, and *d*) Micrographs of nuclear (*Nu*) and cytoplasmic (*Cy*) areas of granulosa cells from a small antral follicle obtained from a 33-d-old rat. The sections were stained with anti-C (*a*), anti-RII (*b*), and anti-RI (*d*) serum. The insets in *b* and *d* are low magnifications; the arrows mark the region of higher magnification. (*a*, *b*, and *d*) Bars, 0.5 μm; × 41,000; (*insets* [*b* and *d*]) bars; 1.0 μm; × 15,000. (*c*) Micrograph of nuclear and cytoplasmic areas of a spermatogonium from a 14-d-old rat stained with anti-C serum. Bar, 1.0 μm; × 22,000.

subunit RII (Fig. 7*b*), and RI (Fig. 7*d*). All three subunits appear to be primarily associated with heterochromatin and perichromatin regions (see, for instance, Fig. 7*b*, arrow) and in areas of the endoplasmic reticulum (Figs. 7, *a* and *b*).

Morphometric Analysis of Subunit Density

Table III lists the subunit densities of spermatogonia from two-wk-old rats and of thecal and granulosa cells from a small antral follicle isolated from the ovary of 33-d-old rats. While thecal cells show a slightly higher RI subunit density, the regulatory subunit RII density is markedly higher in granulosa cells. This is in apparent agreement with biochemical studies in which relatively higher levels of RII than RI were identified in rat granulosa cells (40).

The quantitative evaluation of immunogold labeling over rat hepatocytes from glucagon-treated and partially hepatectomized rats has previously been published (41, 42). A modulation of subunit labeling density was observed in hepatocytes after glucagon administration as well as after partial hepatectomy. After glucagon administration, the labeling density of the catalytic subunit in the nucleus increased about 2.5 to 3-fold and to a lesser degree (1.5- to 1.9-fold) in extranuclear areas. RI and RII labeling densities were, however, not affected by glucagon. Partial hepatectomy elicited a marked increase of staining density of RI and C but not of RII over

TABLE III. *Morphometric Quantitation of cAMP-dependent Protein Kinase Subunit Localization in Rat Ovarian Granulosa and Thecal Cells and Spermatogonia*

Cell type	Staining Intensity (Gold particles/μm^2 ± SEM)					
	Nucleus			Cytoplasm		
	RI	*RII*	*C*	*RI*	*RII*	*C*
Granulosa cells	66.2 ± 2.5	83.6 ± 2.4	162.6 ± 5.7	67.7 ± 3.4	66.6 ± 1.3	70.7 ± 4.0
Thecal cells	81.0 ± 2.7	69.1 ± 5.3	167.6 ± 10.2	73.2 ± 4.6	55.3 ± 4.1	64.6 ± 5.2
Spermatogonia	15.2 ± 0.6	12.7 ± 1.1	111.6 ± 4.3	11.8 ± 1.6	9.6 ± 1.0	49.3 ± 1.2

Tissue sections were fixed in 2.5% glutaraldehyde and processed using the immunogold procedure as described in Materials and Methods. The spermatogonia examined were from the testicular tissues of a 2-wk-old rat. Granulosa and thecal cells were from small antral follicles isolated from 33-d-old rats.

TABLE IV. *Morphometric Quantitation of cAMP-dependent Protein Kinase Subunit Localization in Dibutyryl cAMP-treated H4IIE Hepatoma Cells*

Time after dibutyryl cAMP treatment	Staining Intensity (Gold particles/μm^2 ± SEM)					
	Nucleus			Cytoplasm		
min	*RI*	*RII*	*C*	*RI*	*RII*	*C*
0	13.4 ± 1.6 (6)	27.9 ± 2.9 (5)	143.5 ± 13.8 (6)	31.2 ± 4.7 (6)	26.6 ± 3.8 (4)	34.1 ± 3.5 (6)
2	22.1 ± 1.9 (6)	26.8 ± 1.8 (4)	138.1 ± 7.9 (5)	24.9 ± 0.8 (6)	28.4 ± 2.4 (4)	41.2 ± 3.3 (5)
5	25.6 ± 2.3 (6)	22.1 ± 1.5 (4)	134.8 ± 6.5 (5)	23.3 ± 2.2 (6)	18.3 ± 0.6 (4)	36.7 ± 0.3 (5)
10	20.9 ± 3.3 (5)	63.3 ± 3.6 (7)	248.0 ± 11.1 (6)	20.8 ± 2.8 (5)	34.6 ± 1.6 (7)	41.9 ± 1.6 (6)
15	34.9 ± 2.5 (5)	25.7 ± 1.9 (5)	165.9 ± 16.6 (5)	25.8 ± 2.3 (5)	21.6 ± 1.4 (5)	42.8 ± 5.1 (5)
30	14.1 ± 2.2 (5)	40.4 ± 5.0 (5)	180.9 ± 20.1 (5)	14.9 ± 0.9 (5)	33.4 ± 3.6 (5)	42.2 ± 7.3 (5)
60	25.5 ± 2.6 (6)	31.5 ± 2.5 (5)	164.8 ± 7.2 (6)	17.5 ± 0.8 (6)	19.8 ± 1.3 (5)	50.8 ± 4.4 (6)
120	41.3 ± 5.3 (5)	26.8 ± 1.9 (5)	122.5 ± 11.3 (5)	16.6 ± 1.4 (5)	20.2 ± 0.9 (5)	40.4 ± 4.8 (5)

H4IIE hepatoma cells were stimulated with 0.5 mM dibutyryl cAMP for the time periods indicated. Cells were fixed in 2.5% glutaraldehyde and processed as described in Materials and Methods. The numbers in parentheses represents number of cells analyzed.

the nuclear area. Cytoplasmic staining density was not markedly altered after partial hepatectomy.

Quantitation of the subunit density in dibutyryl cAMP-treated H4IIE hepatoma cells is shown in Table IV. These data allow a comparison of the relative staining densities of each subunit in untreated versus dibutyryl cAMP-treated cells. The staining density of all three subunits changed to varying degrees after dibutyryl cAMP treatment. The nuclear catalytic subunit staining density increased significantly ($p < 0.001$) 10 min (1.7-fold increase) after stimulation. Additionally, the nuclear RI subunit showed an increased labeling at 15 min (2.6-fold increase, $p < 0.01$). RII labeling peaked 10 min (2.3-fold increase, $p < 0.001$) and 30 min (1.5-fold increase, $p < 0.05$) after cyclic nucleotide treatment. There was a slight decrease of cytoplasmic RI subunit staining in the cytoplasm, whereas cytoplasmic RII and C staining did not change significantly.

DISCUSSION

Through the use of a newly developed post-embedding immunogold technique, we have localized all three subunits of cAMP-dependent protein kinase within the nucleus and in extranuclear areas of hepatocytes, ovarian granulosa and thecal cells, spermatogonia, and cultured H4IIE hepatoma cells. Evaluation of the immunogold staining patterns showed that the three subunits are selectively localized over several different nuclear substructures: nucleolus, condensed (hetero) chromatin, interchromatin granules, and perichromatin regions. The specificity of antigen–antibody interaction was carefully evaluated and demonstrated by the ELISA and immunoblot analysis. Immunoblotting is limited to the transfer of soluble protein antigens. Therefore, it is conceivable that insoluble potential cross-reacting antigens are not transferred from the gel to the nitrocellulose membrane. However, we find no indication of this from the autoradiographs (Fig. 2). Controlled studies using preimmune sera or staining of tissue with antisera that had been preadsorbed with purified antigen revealed insignificant nonspecific adsorption of the colloidal gold reagent to any intracellular compartment. In addition, staining of sinusoidal areas of rat liver sections was at background level.

The ultrastructural localization of all three subunits in the nucleus of various cell types was achieved using a colloidal gold–linked second antibody reagent. The immunogold technique has been used previously to investigate the localization of antigen in the nucleus of eukaryotic cells (23–25, 41, 42, 43). Immunogold reagents are ideal probes for localizing antigen–antibody complexes and exhibit distinct advantages over immunofluorescent techniques or conventional stains such as horseradish peroxidase and ferritin. The discrete size of the colloidal gold reagent and the high electron density of gold allows for easy visualization of antibody binding sites over electron-dense regions of the nucleus such as heterochromatin and the nucleolus. Additionally, in contrast to immunofluorescence, immunogold complexes offer a high degree of resolution with a low degree of nonspecific staining and allow a semi-quantitative evaluation of staining density. The availability of differing sizes of colloidal gold–linked secondary antibody has allowed for the design of experiments using more than one antiserum label. Thus, we are presently defining the exact spatial relationships of the RI, RII, and C

subunits within the nucleus.

Optimal nuclear immunolabeling with an acceptably preserved nuclear ultrastructure was obtained with 2.5% glutaraldehyde as fixative and a low viscosity embedding resin. Under these experimental conditions the three nuclear subunits are relatively resistant to the destructive potential of fixation, dehydration, and embedding. Cytoplasmic labeling is similarly optimal under these experimental conditions. However, direct quantitative comparisons between nuclear and cytoplasmic subunit staining density should be done with caution. Possible differences of the binding affinities of the protein kinase subunits to nuclear substructures and to extranuclear regions, and a possible preferential loss of cytoplasmic antibody during tissue processing, may make these comparisons imprecise. Also, because of differing antibody–antigen affinities, a direct comparison of the labeling densities of the individual subunits should be done with caution.

Quantitative evaluation of the immunogold staining patterns by morphometric analysis demonstrated several notable changes of nuclear antigen labeling densities at times of cellular stimulation by effector agents. As we have previously shown, glucagon stimulation elicited an increased nuclear staining of only the catalytic subunit (41), whereas the staining density of both the nuclear catalytic and regulatory subunit RI was increased 16 h after partial hepatectomy (42). In the present study, we additionally demonstrated that dibutyryl cAMP treatment of H4IIE hepatoma cells leads to a modulation of nuclear RI, RII, and C subunit densities (see Table IV).

The altered staining densities of the nuclear cAMP–dependent protein kinase subunits that occurred in response to partial hepatectomy correlate well with the observed subunit modulation during the prereplicative phase of rat liver regeneration identified by biochemical and immunochemical measurements (7). Similarly, glucagon treatment of rats has been shown to increase the nuclear activity level of catalytic subunit (44, 45).

Several factors may be responsible for the changing antigen densities. Firstly, the increased nuclear staining density is most likely the result of a net increase of antigen molecules in the nucleus as the consequence of translocation of antigen from extranuclear sites into the nucleus (46). The localization of antigen over nuclear substructures and cytoplasm and changing antigen densities in the nucleus may indicate that the antigens shuttle between nuclear and cytoplasmic structures and that this may play an important functional role in nuclear–cytoplasmic communication. Secondly, although the RI, RII, and C-antisera used in our studies have identical affinities for their comlementary antigen in either the nondissociated holoenzyme form or in the dissociated form as identified by the ELISA (34, 35), they could conceivably interact only with the dissociated subunits in tissue sections. Should this be the case, increased staining density would occur after cellular stimulation reflecting the formation of free subunits as the result of cAMP-mediated dissociation of the cAMP-dependent protein kinase holoenzymes. However, we did not observe a concomitant modulation of cytoplasmic staining density which, therefore, makes this latter possibility unlikely.

In conclusion, the aim of the present study has been directed toward the immunocytochemical identification of the unique nuclear sites of RI, RII, and C subunit binding using specific antisera and immunogold electron microscopy. The results reported here demonstrate the usefulness of immunogold reagents in the cytochemical study of cAMP-dependent protein kinase subunits and extend earlier work on nuclear cAMP-dependent protein kinase subunit localization using immunofluorescence at the light microscopy level (47–49). The technique appears sensitive and specific and the resolution allows a precise correlation between antigen and antigenic binding sites. Potential applications of this technique are numerous, particularly for the identification of the nuclear sites of action of the cAMP-dependent protein kinase subunits under a variety of physiological conditions.

We thank Ms. L. Evely for her excellent technical assistance.

This work was supported in part by grants GM 23895 and HD 12046 from the National Institutes of Health. Stephen P. Squinto is the recipient of a National Institutes of Health Postdoctoral Fellowship (GM 09752).

Received for publication 4 December 1984, and in revised form 8 May 1985.

REFERENCES

1. Maurer, R. A. 1981. Transcriptional regulation of the prolactin gene by ergocryptine and cyclic AMP. *Nature (Lond.)* 294:94–97.
2. Lamers, W. H., R. W. Hanson, and H. M. Meisner. 1982. cAMP stimulates transcription of the gene for cytosolic phosphoenolpyruvate carboxykinase in rat liver nuclei. *Proc. Natl. Acad. Sci. USA* 79:5137–5141.
3. Jungmann, R. A., D. C. Kelley, M. F. Miles, and D. M. Milkowski. 1983. Cyclic AMP regulation of lactate dehydrogenase. *J. Biol. Chem.* 258:5312–5318.
4. Murdoch, G. H., R. Franco, R. M. Evans, and M. G. Rosenfeld. 1983. Polypeptide hormone regulation of gene expression. *J. Biol. Chem.* 258:15329–15335.
5. Rubin, C. S., and O. M. Rosen. 1975. Protein phosphorylation. *Annu. Rev. Biochem.* 44:831–887.
6. Johnson, E. M. 1977. Cyclic AMP-dependent protein kinase and its nuclear substrate proteins. *Adv. Cyclic Nucleotide Res.* 8:267–310.
7. Laks, M. S., J. J. Harrison, G. Schwoch, and R. A. Jungmann. 1981. Modulation of nuclear protein kinase activity and phosphorylation of histone H1 subspecies during the prereplicative phase of rat liver regeneration. *J. Biol. Chem.* 256:8775–8785.
8. Corbin, J. D., S. L. Keely, and C. R. Park. 1975. The distribution and dissociation of cyclic adenosine 3′,5′-monophosphate-dependent protein kinases in adipose, cardiac and other tissues. *J. Biol. Chem.* 250:218–225.
9. Builder, S. E., J. A. Beavo, and E. G. Krebs. 1980. Stoichiometry of cAMP and 1,N^6-etheno-cAMP binding to protein kinase. *J. Biol. Chem.* 255:2350–2354.
10. Corbin, J. D., P. H. Sudgen, L. West, D. A. Flockhart, T. N. Lincoln, and D. McCarthy. 1978. Studies on the properties and mode of action of the purified regulatory subunit of bovine heart adenosine 3′,5′-monophosphate-dependent protein kinase. *J. Biol. Chem.* 253:3997–4003.
11. Jungmann, R. A., and D. H. Russell. 1977. Cyclic AMP, cyclic AMP-dependent protein kinase, and the regulation of gene expression. *Life Sci.* 20:1787–1798.
12. Lee, P. C, D. Radloff, J. S. Schweppe, and R. A. Jungmann. 1976. Testicular protein kinase: characterization of multiple forms and ontogeny. *J. Biol. Chem.* 251:914–921.
13. Eppenberger, U., W. Roos, D. Fabbro, A. Sury, J. Weber, E. Bechtel, P. Huber, and R. A. Jungmann. 1979. Ontogeny of the adenosine-3′,5′-phosphate-dependent protein-kinase system during early uterine development. *Eur. J. Biochem.* 98:253–259.
14. Malkinson, A. M., and M. S. Butley. 1981. Alterations in cyclic adenosine 3′,5′-monophosphate-dependent protein kinases during normal and neoplastic lung development. *Cancer Res.* 41:1334–1341.
15. Ledinko, N., and I. J. A. Chan. 1984. Increase in type I cyclic adenosine 3′:5′-monophosphate-dependent protein kinase activity and specific accumulation of type I regulatory subunits in adenovirus type 12-transformed cells. *Cancer Res.* 44:2622–2627.
16. Hunzicker-Dunn, M., R. A. Jungmann, L. Evely, G. L. Hadawi, E. T. Maizels, and D. E. West. 1984. Modulation of soluble ovarian adenosine 3′,5′-monophosphate-dependent protein kinase activity during prepubertal development of the rat. *Endocrinology.* 115:302–311.
17. Faulk, W. P., and G. M. Taylor. 1971. An immunocolloid method for the electron microscope. *Immunochemistry.* 8:1081–1083.
18. Roth, H., M. Bendayan, and L. Orci. 1978. Ultrastructural localization of intracellular antigens by the use of protein A–gold complex. *J. Histochem. Cytochem.* 26:1074–1081.
19. Bendayan, M., J. Roth, A. Perrelet, and L. Orci. 1980. Quantitative immunocytochemical localization of pancreatic secretory protein in subcellular compartments of rat acinar cell. *J. Histochem. Cytochem.* 28:149–160.
20. Geuze, H. J., J. W. Slot, P. A. VanderLey, and R. C. T. Scheffner. 1981. Use of colloidal gold particles in double-labeling immunoelectron microscopy of ultrathin frozen tissue sections. *J. Cell Biol.* 89:653–665.
21. Slot, J. W., and H. J. Geuze. 1981. Sizing of protein A–collodial gold probes for immunoelectron microscopy. *J. Cell Biol.* 90:533–536.
22. Warchol, J. B., R. Brelinska, and D. C. Herbert. 1982. Analysis of colloidal gold methods for labelling proteins. *Histochemistry.* 76:567–575.
23. Mace, M. L., Jr., N. T. Van, and P. M. Conn. 1977. Electron microscopic localization of DNA-dependent RNA polymerase binding sites on DNA using enzyme immobilized on colloidal gold. *Cell Biol. Int. Rep.* 1:527–533.
24. Bendayan, M. 1981. Ultrastructural localization of nucleic acids by the use of enzyme-gold complexes. *J. Histochem. Cytochem.* 29:531–541.
25. Clevenger, C. V., and A. L. Epstein. 1984. Use of immunogold electron microscopy and monoclonal antibodies in the identification of nuclear substructures. *J. Histochem. Cytochem.* 32:757–765.

26. Spurr, A. R. 1969. A low-viscosity epoxy resin embedding medium for electron microscopy. *Ultrastruct. Res.* 26:31–42.
27. Bendayan, M. 1982. Double immunocytochemical labeling applying the protein A-gold technique. *J. Histochem. Cytochem.* 30:81–85.
28. Bendayan, M., and M. Zollinger. 1983. Ultrastructural localization of antigenic sites on osmium-fixed tissues applying the protein A-gold technique. *J. Histochem. Cytochem.* 31:101–109.
29. DeMay, J. 1983. A critical review of light and electron microscopic immunocytochemical techniques used in neurobiology. *J. Neurosci. Methods.* 7:1–18.
30. Erlandsen, S. L., J. A. Parsons, and C. B. Rodning. 1979. Technical parameters of immunostaining of osmicated tissue in epoxy sections. *J. Histochem. Cytochem.* 27:1286–1289.
31. Baskin, D. G., S. L. Erlandsen, and J. A. Parsons. 1979. Influence of hydrogen peroxide or alcoholic sodium hydroxide on the immunocytochemical detection of growth hormone and prolactin after osmium fixation. *J. Histochem. Cytochem.* 27:1290–1292.
32. Renolds, E. S. 1963. The use of lead citrate at high pH as an electron-opaque stain in electron microscopy. *J. Cell Biol.* 17:208–212.
33. Dills, W. L., C. D. Godwin, T. M. Lincoln, J. A. Bechtel, J. D. Corbin, and E. G. Krebs. 1979. Purification of cyclic nucleotide receptor proteins by cyclic nucleotide affinity chromatography. *Adv. Cyclic Nucleotide Res.* 10:199–217.
34. Schwoch, G., A. Hammann, and H. Hilz. 1980. Antiserum against the catalytic subunit of cAMP-dependent protein kinase. *Biochem. J.* 192:223–230.
35. Schwoch, G., and A. Hammann. 1982. Determination and comparative analysis of the catalytic subunit of adenosine 3′,5′-cyclic phosphate-dependent protein kinase by an enzyme-linked immunosorbent assay. *Biochem. J.* 208:109–117.
36. Miles, M. F., P. Hung, and R. A. Jungmann. 1981. Cyclic AMP regulation of lactate dehydrogenase M-subunit mRNA in isoproterenol and N^6,$O^{2'}$-dibutyryl cyclic AMP-stimulated rat C6 glioma cells by hybridization analysis using a cloned cDNA probe. *J. Biol. Chem.* 256:12545–12552.
37. Ouchterlony, O. 1968. Handbook of immunodiffusion and immunoelectrophoresis. Ann Arbor Scientific Publishers, Ann Arbor, MI. 1–500.
38. Towbin, H., T. Staehelin, and J. Gordon. 1979. Electrophoretic transfer of proteins from polyacrylamide gels to nitrocellulose sheets: procedure and some applications. *Proc. Natl. Acad. Sci. USA* 76:4350–4354.
39. Laemmli, U. K. 1970. Cleavage of structural protein during the assembly of the head of bacteriophage T4. *Nature (Lond.).* 227:680–685.
40. Richards, J. S., N. Sehgal, and J. S. Tash. 1983. Changes in content and cAMP-dependent phosphorylation of specific proteins in granulosa cells of preantral and preovulatory ovarian follicles and in corpora lutea. *J. Biol. Chem.* 258:5227–5232.
41. Kuettel, M. R., G. Schwoch, and R. A. Jungman. 1985. Localization of cyclic AMP-dependent protein kinase subunits in rat hepotocyte nuclei by immunogold electron microscopy. *Cell Biol. Int. Rep.* 8:949–957.
42. Squinto, S. P., D. C. Kelley-Geraghty, M. R. Kuettel, and R. A. Jungmann. 1985. Ultrastructural localization of cAMP-dependent protein kinase subunits in regenerating rat hepotocytes using immunogold electron microscopy. *J. Cyclic Nucleot. Protein Phosphorylation Res.* 10:65–73.
43. Clevenger, C. V., and A. L. Epstein. 1984. Identification of a nuclear protein component of interchromatin granules using a monoclonal antibody and immunogold electron microscopy. *Exp. Cell Res.* 151:194–207.
44. Higashino, H., and M. Takeda. 1974. Changes in adenosine 3′,5′-monophosphate level and protein kinase activity by glucagon in rat liver nuclei. *J. Biochem.* 75:189–191.
45. Palmer, W. K., M. Castagna, and D. A. Walsh. 1974. Nuclear protein kinase activity in glucagon-stimulated perfused rat livers. *Biochem. J.* 143:469–471.
46. Jungmann, R. A., and E. G. Kranias. 1977. Nuclear phosphoprotein kinases and the regulation of gene transcription. *Int. J. Biochem.* 8:819–830.
47. Steiner, A. L., Y. Koide, H. S. Earp, P. J. Bechtel, and J. A. Beavo. 1978. Compartmentalization of cyclic nucleotides and cyclic AMP-dependent protein kinases in rat liver: immunocytochemical demonstration. *Adv. Cyclic Nucleotide Res.* 9:691–706.
48. Byus, C. V., and W. H. Fletcher. 1982. Direct cytochemical localization of catalytic subunits dissociated from cAMP-dependent protein kinase in Reuber H-35 hepatoma cells. II. Temporal and spatial kinetics. *J. Cell Biol.* 93:727–734.
49. Van Sande, J., H. L. Huang, A. Steiner, and J. E. Dumont. 1983. Immunocytochemical localization of protein kinases and calmodulin in dog thyroid cells. *Cell Biol. Int. Rep.* 7:981–988.